Iranian Journal of Fuzzy Systems

Volume 19, Number 1, (2022), pp. 31-45

Original paper

University of Sistan and Baluchestan

Type 2 adaptive fuzzy control approach applied to variable speed DFIG based wind turbines with MPPT algorithm

S. M. Hosseini[1] and M. Manthouri[2]

[1,2] *Electrical and Electronic Engineering Department, Shahed University, Tehran, Iran*

hosseinimo92@ieee.org, mmanthouri@shahed.ac.ir

Abstract

In this research, a Type 2 adaptive fuzzy controller approach is formulated and designed to be applied to variable speed doubly fed induction generator-based wind turbines directly connected to the grid. It brings this study to evaluate the whole operation of the system to capture the highest rate of power in the wind turbines. The controlling approach is considered to keep the stator reactive power to the ideal value. In contrast to the other researches, here the controlling technique is developed through the nonlinear systems. By the aim of making progress in system operation, in contrast with the Type 1 adaptive fuzzy system, type two adaptive fuzzy theory is proposed to approximate a large number of uncertainties and the dynamic nonlinearities, exists in tracking errors which may limit the system performance. Feedback linearization control approach helps us to algebraically alter the system into a linearized plant. Thanks to the Lyapunov theorem, the introduced type two adaptive fuzzy approach is proved to meet the uniformly ultimately boundness (UUB) property. On the other hand, it results better tracking function. The simulation outputs represent that the proposed technique is robust enough in presence of parameter variations and unstructured uncertainties.

Keywords: Adaptive, Type 2 fuzzy, DFIG, wind turbine, variable speed.

1 Introduction

The highest extracted power is held by various control schemes. One of these methods is the neural controller, the flexibility of this controller may optimize the functioning of the plant, as a result, the reference voltages converge to optimal values [26] , A real-time neural sliding mode field-oriented control idea, designed for a DFIG based wind turbine to keep the power factor at nominal levels, and help the stator active and reactive powers to track the desired values [18]. Taking into consideration that different types of SMCs like high order sliding mode can handle a wide range of uncertainties and disturbances [19], it results in some aspects such as chattering-free behavior, finite reaching time, and robustness [11] otherwise it can bring the plant to control or track the torque for achieving highest produced power [6, 17]. Despite tuning the tip speed ratio based on the optimal values, the system cant capture elevated energy values, so implementing a high order sliding mode method as a power regulator can gain fault tolerance to extract the maximum power values [3]. The other solution for this problem is derived from an observer-based combination of three controllers such as polynomial RST, LQG to follow the optimums [23]. The second-order sliding mode control is employed for different aims. In a study, SOSM satisfies free chattering behavior, acquiring finite reaching time and robustness in the presence of disturbances and unmodeled dynamics [4]. On the other application, A combination of a SOSM and a super twisting algorithm adjusts the reactive power of the stator and it may increase the possibility of finite-time stabilization [8]. The fuzzy controller is one of the methods which may optimize the performance of the methodology. In a case, it is applied to encounter stator and internal dynamics to meet MPPT targets [29], Moreover, to remove the chattering, caused by discontinuous control signals, a fuzzy control system can adequately resolve this matter in the existence of a sliding mode control system [25]. The proportional and integral (PI) controller is one

Corresponding Author: M. Manthouri

Received: December 2019; Revised: November 2020; Accepted: May 2021.

https://doi.org/10.22111/IJFS.2022.6549

of the methods to reject the uncertainties and disturbances, and tuning the related gains are met by utilizing swarm optimization, genetic algorithm, artificial intelligence, and gain scheduling methods. The PI technique can be replaced with FIS in rotor speed, stator active and reactive power controls. For DC link voltage control, it is offered to apply a fuzzy logic gain tuner to update the PI controller to yield a robust performance [27]. The combination of an adaptive system and fuzzy control is analyzed for many cases. In PMSMs, for speed tracking, an adaptive fuzzy control provides robustness in the system with structured and unstructured uncertainties [15], if the above approach being configurated as an estimator of nonlinearities, the backstepping procedure helps to increase the possibility of optimal and robust responses [13]. Furthermore, a robust adaptive control design is suggested to regulate a class of nonlinear system with parametric uncertainties and unknown nonlinearities arise by modeling errors, disturbances, and time changes based on triangular bounds assumption [24]. A controller based on SMC, Interval type 2 fuzzy logic system as an estimator and adaptive control system in non-stationary condition, encounters all types uncertainties, and human expert knowledge holds a crucial part of the design [20], Unless, all these methods may need to simplify the DFIG model, but a nonlinear state feedback control can do the trick for both generator control and aero turbine control. This model will grow the system efficiency, as the two separated controllers are designed for both generator and aero turbine control [5]. In addition, to overcome the simplifying assumptions, designers can use a nonlinear state feedback controller, consisted of both DFIG control and aero turbine predictive control on low speed region. The whole control approach leads to a development in the trade-off between efficiency and complexity [2].

2 Wind turbine scheme

A simple structure of doubly fed induction generator-based wind turbine is shown in Figure 1 The wind turbine propeller is connected to gearbox and then by a non-rigid shaft, it is assembled to the doubly fed induction generator. This system comprises two parts: The rotor and the stator. As the gearbox is connected to the rotor winding of DFIG by means of a non-rigid shaft which is supplied with a two directional converter, the stator winding is directly linked to the grid. In this paper, the amplitude and the position of rotor voltage vector is considered to be tuned.

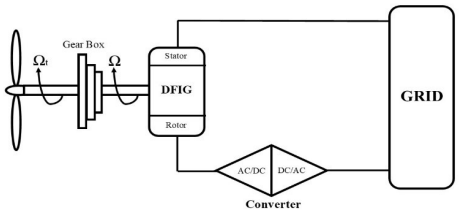

Figure 1: Simplified DFIG based wind turbine.

The aerodynamic power or so-called mechanical power extracted by the WT can be formulated as below [4, 7, 29] and all parameters and variables can be found in Tables 1 and 2

$$P_p = 0.5\mathcal{P}\pi R^2 C_p(\lambda,\beta){v_r}^3. \tag{1}$$

For a wind turbine with fixed pitch angle, maximum theorical value of $C_p(\lambda,\beta)$ according to the Betz limit, the tip-speed ratio will reach to a unique peak point λ_{peak}. In this study, to maximize the value of C_p, given by (2), the power coefficient can be chosen as below [21, 30].

$$C_p(\lambda,\beta) = c_1\left(c_2 n - c_3\beta - c_4\right)e^{-c_5 n} + c_6\lambda. \tag{2}$$

$$n = \frac{1}{\lambda + c_7\beta} - \frac{c_8}{\beta^3+1}.$$

$$c_1 = 0.5176\ ,\ c_2 = 116\ ,\ c_3 = 0.4\ ,\ c_4 = 5\ ,\ c_5 = 21\ ,\ c_6 = 0.0068\ ,\ c_7 = 0.08\ ,\ c_8 = 0.035.$$

The tip speed ratio (λ) plays a key role in formulating the aerodynamic torque $\mathcal{T}_{ar}$, based on the following formula,

$$\lambda = \frac{R\Omega_t}{v_r} = \frac{R\Omega}{Gv_r}. \tag{3}$$

In which, R, Ω and G determines in order, the rotor radius, the generator speed and transmission ratio in gear box. Here, δ is named as the total coefficient of leakage flux.

$$\mathcal{T}_{ar} = \frac{P_p}{\Omega_{total}} = \frac{1}{\lambda^3}\mathcal{P}R^5\pi C_p(\lambda,\beta)\Omega_t^2. \tag{4}$$

$$\delta = (1 - \left(\frac{M^2}{L_r L_s}\right)).$$

Table 1: Parameters used to calculate the aerodynamic torque

Parameter	Value	Name
C_{p-max}	0.48	Max power coefficient
P	1.221	Air density
β	2°	Blade pitch angle
λ_{peak}	8.1	Tip speed ratio

2-1) Doubly Fed induction generator and mechanical Dynamics representation:
This system contains some parameters as below:
R: resistance, L: inductance, M: Mutual inductance, V: Voltage, I: Current, Ψ : flux, θ_s : electrical angles of stator, θ_r: electrical angles of rotor, θ_m: rotor mechanical position $\omega_s = \frac{d\theta_s}{dt}$, $\omega_r = \frac{d\theta_r}{dt}$, $\omega = \frac{d\theta_m}{dt}$: stator, rotor and shaft electrical frequencies The equations of dynamic model for DFIG in a random rotating d-q frame is expressed as (The indexed s and r indicate stator and rotor and also d-q is related to synchronous reference frame indices)

$$\begin{cases} \dot{V}_{s_d} = \dot{\psi}_{s_d} - \omega_s\psi_{s_q} + R_s I_{s_d} \\ \dot{V}_{s_q} = \dot{\psi}_{s_q} - \omega_s\psi_{s_d} + R_s I_{s_q} \\ \dot{V}_{r_d} = \dot{\psi}_{r_d} - \omega_r\psi_{r_q} + R_r I_{r_d} \\ \dot{V}_{r_q} = \dot{\psi}_{r_q} - \omega_r\psi_{r_d} + R_r I_{r_q} \end{cases} \tag{5}$$

And the d-q stator/rotor fluxes are calculated through:

$$\begin{cases} \psi_{s_d} = MI_{r_d} + L_s I_{s_d} \\ \psi_{s_q} = MI_{r_q} + L_s I_{s_q} \\ \psi_{r_d} = MI_{s_d} + L_r I_{r_d} \\ \psi_{r_q} = MI_{s_q} + L_r I_{r_q} \end{cases} \tag{6}$$

By use of the previous parameters, the active and reactive powers are reckoned through the following stated formulas:

$$\begin{cases} P_s = 1.5(V_{s_d} I_{s_d} + V_{s_q} I_{s_q}) \\ Q_s = 1.5(V_{s_q} I_{s_d} - V_{s_d} I_{s_q}) \end{cases} \tag{7}$$

Inspiring form [7], the mechanical dynamics are illustrated by

$$\mathcal{H}_t\Omega = \mathcal{T}_{ar} - \mathcal{T}_{el} - \mathcal{T}_{fr}. \tag{8}$$

It must be mentioned that the generator total inertia in wind turbine, named as $mathcal H_t$ is propelled by aerodynamic torque $\mathcal{T}_{ar}$ and decelerated by electromagnetic torque $\mathcal{T}_{el}$ when it augments and, $\mathcal{T}_{fr}$ as friction torque is going to be discussed and formulated in following sections. The electromagnetic torque is calculated by

$$\mathcal{T}_{el} = PML_s(\psi_{s_q} I_{r_d} - \psi_{s_d} I_{r_q}). \tag{9}$$

P:Pair pole number in DFIG

According to [15], in complicated systems such as WTs, using a friction scheme, consists of friction terms such as μ_{cmb}: Coulomb, μ_{vis}: viscous and μ_{stc}: static, provide in (10)

$$\mathcal{T}_{fr} = sign\,(\Omega)\,(\mu_{cmb} + \ \mu_{stc} e^{-(\frac{\Omega}{\eta_s})^2}) + \mu_{vis}\Omega. \tag{10}$$

Remark 2.1. *It is represented in Figure 2 that the above offered friction model depicts more accurate behavior of DFIMs, in contrast it enters solid nonlinear terms to the system* [15].

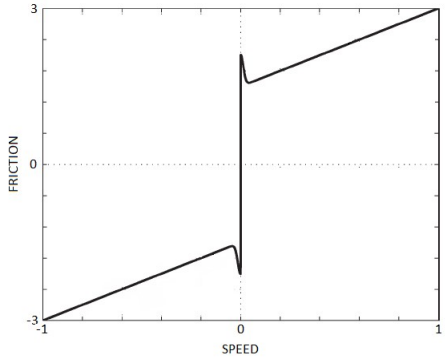

Figure 2: General behavior of friction model.

The main drawback in the general behavior of friction model is explained by the unspecified force values at zero-speed which might be solved by some small changes in the friction torque function, the sign function substitute with Tanh function [1].

$$\mathcal{T}_{fr} = Tanh\,(\Omega)\,(\mu_{cmb} + \mu_{stc} e^{-(\frac{\Omega}{\eta_s})^2}) + \mu_{vis}\Omega. \tag{11}$$

Having d-axis aligned with stator flux axis due to the Park transformation, we use $\Psi_{sq} = 0$ and $\Psi_{sd} = \Psi_s$ [22], regardless of the stator resistance in high power generators applied to wind turbines, the equations (5) will be changed as following:

$$\begin{cases} V_{s_d} = \psi_{s_d} = \psi_s \rightarrow V_{s_d} = 0 \\ V_{s_q} = \Omega_s \psi_{s_d} \rightarrow V_{s_q} = \Omega_s \psi_s \end{cases} \tag{12}$$

Assuming voltage amplitude in stator V_s and the frequency ω_s as constant values (12), the stator reactive power and the electromagnetic torque equations are modified as (13), (14):

$$\mathcal{T}_{el} = -P\frac{M\psi_s}{L_s} I_{r_q}. \tag{13}$$

$$Q_s = \frac{1.5V_s}{L_s}(\Psi_s - MI_{rd}). \tag{14}$$

Now we can define the states of the wind turbine system:

$$\begin{cases} \dot{I}_{r_d} = -gI_{r_d} + (\omega_s - \rho\Omega)I_{r_q} + \alpha\beta\psi_s + \delta^{-1}V_{r_d} \\ \dot{I}_{r_q} = -gI_{r_q} + (\omega_s - \rho\Omega)I_{r_d} + \beta\psi_s\rho\Omega - \beta V_s + \delta^{-1}V_{r_q} \\ \dot{\Omega} = \mathcal{H}_t^{-1}(\mathcal{T}_{ar} - \mathcal{T}_{el} - \mathcal{T}_{fr}) \end{cases} \tag{15}$$

$$\begin{cases} S_d(x) = -gI_{r_d} + (\omega_s - \rho\Omega)I_{r_q} + \alpha\beta\psi_s \\ S_q(x) = -gI_{r_q} + (\omega_s - \rho\Omega)I_{r_d} + \beta\psi_s\rho\Omega - \beta V_s \end{cases} \tag{16}$$

Noting the terms $\alpha = \frac{R_s}{L_s}$, $\beta = \frac{M}{\delta L_s}$, $g = (\frac{R_r}{\delta} + \alpha\beta M)$ and substituting (16) in (15), the state equations turn to

$$\begin{cases} \dot{I}_{r_d} = S_d(x) + \delta^{-1}V_{r_d} \\ \dot{I}_{r_q} = S_q(x) + \delta^{-1}V_{r_q} \\ \dot{\Omega} = \mathcal{H}_t^{-1}(\mathcal{T}_{ar} - \mathcal{T}_{el} - \mathcal{T}_{fr}) \end{cases} \tag{17}$$

3 The control approach for the doubly fed induction generator-based wind turbine

The operation of wind turbines is classified into three zones, this classification is conducted by the wind speed v and the extracted power P, as represented in Figure 3 [4]. A brief description is provided to express the behavior of the system in each zone: Zone 1: In this region, the wind speed is not strong enough to make the wind turbine spin. Zone 2: As wind speed increases, it gradually initiates to spin to produce the maximum extracted power. here, the maximum power can be obtained by applying a speed controlling technique to the plant. In this region, electromagnetic torque control plays a key role in the fixed pitch angle setting.

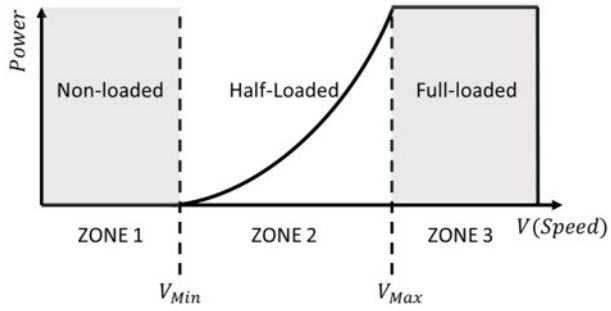

Figure 3: Wind turbine working zones

To approach the maximum power extracted, in spite of the variations of wind speed, the rotor speed is monitored to maintain the optimum value of the tip speed ratio λ_{opt}. On the other hand, C_P has to stay at the maximum point ($C_{p_{max}}$). So, the aerodynamic torque is calculated by

$$\mathcal{T}_{ar-opt} = \frac{0.5}{\lambda^3{}_{opt}} \rho R^5 \pi C_{pmax} \Omega_t^2. \tag{18}$$

Having $\varrho = \frac{1}{2\lambda^3{}_{opt}} \rho \pi R^5 C_{p_max}$ and $\Omega_t = \frac{\Omega}{G}$, the aerodynamic torque can be rewritten as,

$$\mathcal{T}_{ar-opt} = \varrho \Omega_t^2.$$

For keeping the system on working in maximum extracted power range, the electromagnetic torque $\mathcal{T}_{el}$ has to follow the optimal aerodynamic torque $\mathcal{T}_{ar_Opt}$. If we consider $Q_s = 0$, the unitary power factor requirement is met, therefore we can select the following equation:

$$I_{rd_i dl} = \frac{V_s}{\omega_s M} \tag{19}$$

4 Type 2 adaptive fuzzy control approach

In Figure 4 the provided diagram, describes the structure of type 2 fuzzy logic system.

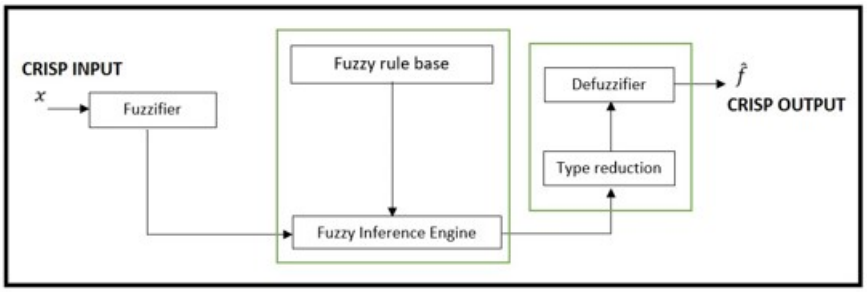

Figure 4: Basic type 2 fuzzy logic system

A type 2 fuzzy logic system consists of n inputs, $x_1 \in X_1, , x_n \in X_n$ constituting a vector $x^T = [x_1, x_2, \ldots, x_n]$ resulting in a singleton output $\hat{f} \in F$. $(\bar{x}, \hat{f} \in R^n)$. The fuzzy rule will be formed as

$$Rule^{(r)} : \text{IF } x_1 \text{ is } \widetilde{B}_1^r \text{ and} \ldots . \text{ and } x_n \; is \; \widetilde{B}_n^r \text{ THEN } \hat{f} \text{ is } \widetilde{f}^r.$$

$B_1^r, B_2^r., B_n^r$ are called fuzzy sets and this fuzzy rule depicts a type 2 fuzzy relationship between the input space $x_1 * x_2 * x_3 * \ldots . * \; X_r$ and the output space denoted F, then the membership functions of the above proposed type 2 system is selected as $\mu_{\widetilde{B}_1^r} \times \ldots . \times \mu_{\widetilde{B}_n^r} \rightarrow \widetilde{F}_n^r(x, \hat{f})$. By the purpose of calculating the output of the system, the Nie-Tan method returns

$$\hat{f}(x) = \frac{\sum_{r=1}^{m} \prod_{j=1}^{n} f_r^L \mu_{B_j^i}^L (x_j) + \sum_{r=1}^{m} \prod_{j=1}^{n} f_r^R \mu_{B_j^r}^R (x_j)}{\sum_{r=1}^{m} \prod_{j=1}^{n} \mu_{B_j^r}^L (x_j) + \sum_{r=1}^{m} \prod_{j=1}^{n} \mu_{B_j^r}^R (x_j)}. \tag{20}$$

The output is calculated by singleton fuzzier, product inference, and center-average defuzzifer, at which : The Output of type 2 fuzzy logic system, $\mu_{B_j^i}^{L,R}(x_j)$: The degree of membership of x_j to B_j^i, m : the number of rules. The presented equation (21), can be reformulated for determining fuzzy basis function

$$\hat{f}(x) = \theta^T \psi (x) . \tag{21}$$

In type 2 fuzzy logic system, the vector of adjustable parameter is considered for both Right and Left membership functions $\theta_R^T = [f_1^R, \; f_2^R, \ldots, f_m^R], \theta_L^T = [f_1^L, \; f_2^L, \ldots, f_m^L], \theta^T = [\theta_R^T \quad \theta_L^T]$ then and the same happens to fuzzy basis function as $\psi_R^T = [\psi_{1R}, \psi_{2R}, \ldots . , \psi_{mR}], \psi_L^T = [\psi_{1L}, \psi_{2L}, \ldots . , \psi_{mL}] \psi^T (x) = [\psi_R^T \quad \psi_L^T]$ and this is a fuzzy basis function set with

$$\psi_{i(R,L)} = \frac{\prod_{j=1}^{n} \mu_{B_j^i}^{(L,R)} (x_j)}{\sum_{r=1}^{m} \prod_{j=1}^{n} \mu_{B_j^r}^{(L,R)} (x_j) + \sum_{r=1}^{m} \prod_{j=1}^{n} \mu_{B_j^r}^{(L,R)} (x_j)}. \tag{22}$$

On the next calculation in this study, based on [13], [12], it is supposed that for selected FBFs, at least one rule is active. By applying the universal approximation theory [16, 28], the system $\hat{f}(x)$ approximates a smooth nonlinear function f. In this study, the construction of fuzzy system and membership function is properly defined and the consequent parameter denoted θ is determined by adaptation technique. The doubly fed induction generator-based wind turbines are controlled by the purpose of extracting optimal amount of energy when the optimal aerodynamic torque tracks d-axis rotor reference current via rotor windings voltages as the physical inputs of this system. Theorem: For the input vectors X_1 and X_2, if the tracking errors defined by (23), (24) are employed in the state equations (18), and having the feedback linearization control approach (29), (30) and providing the adaptive laws (34) − (39),

$$X_1 = [I_{rd}, I_{rq}, \Omega, \mathcal{T}_{ar-opt}]^T , X_2 = [I_{rd}, I_{rq}, \Omega, I_{rd_i dl}]^T .$$

$$\mathcal{E}_1 = \mathcal{T}_{el} - \mathcal{T}_{ar-opt}. \tag{23}$$

$$\mathcal{E}_2 = I_{rd} - I_{rd_i dl}. \tag{24}$$

After differentiating the above tracking errors in (25), (26), we get the following equations in accordance with the prior calculations,

$$\dot{\mathcal{E}}_1 = -\frac{PM\psi_s}{L_s}(-gI_{rq} - (\omega_s - \rho\Omega)I_{rd} + \beta\Psi_s\rho\Omega - \beta.V_s - \delta^{-1}V_{rq}) - \dot{\mathcal{T}}_{ar-opt}. \tag{25}$$

$$\dot{\mathcal{E}}_2 = (-gI_{rd} + (\omega_s - \rho\Omega)I_{rq} + \alpha\beta\psi_s + \delta^{-1}V_{rd}) - \dot{I}_{rd_i dl}. \tag{26}$$

Then we can rewrite these two equations:

$$\dot{\mathcal{E}}_1 = S_1(x_1) + N_1 V_{rq}. \tag{27}$$

$$\dot{\mathcal{E}}_2 = S_2(x_2) + N_2 V_{rd}. \tag{28}$$

At which

$$\begin{aligned} S_1(x_1) &= -\frac{PM\varphi_s}{L_s}\left(-gI_{rq} - (\omega_s - \rho\Omega) I_{rd} + \beta\psi_s\rho\Omega - \beta.V_s\right) - \dot{\mathcal{T}}_{ar-opt}, \\ S_2(x_2) &= (-gI_{rd} + (\omega_s - \rho\Omega) I_{rq} + \alpha\beta\psi_s) - \dot{I}_{rd_i dl}, \\ N_1 &= -\frac{PM\psi_s}{L_s}\delta^{-1} \quad , \quad N_2 = \delta^{-1}. \end{aligned}$$

Applying feedback linearization controlling (FLC) approach (29), (30), with known $S_i(x_i)$ and $N_{i=1,2}$ and also state vectors $x_{i=1,2}$ lead us to choose control laws as

$$V_{rq} = N_1^{-1}(-S_1(x_1) - \mathcal{F}_q\mathcal{E}_1\ ) \qquad \mathcal{F}_q > 0, \tag{29}$$

$$V_{rd} = N_2^{-1}(-S_2(x_2) - \mathcal{F}_q\mathcal{E}_2) \qquad \mathcal{F}_d > 0, \tag{30}$$

In these controllers, the nonlinear dynamics parameters must be precisely known. But this issue is not practically possible in doubly fed induction generator-based wind turbine system. Unless this controller cant satisfy the preferred control operation due to unstructured uncertain dynamics, external disturbances and variations in parameters. As a solution adaptive fuzzy system meets the expectancies, by approximating the unknown nonlinear dynamics in tracking error equations. To reach the ideal results, and for constant stator voltage amplitude, frequency constant and unknown machine parameters, it is necessary to measure the speed, rotor currents and stator voltages. In this article, this referred feature

$$0 < |\mathcal{E}_i| - \mathcal{E}_i Tanh(\frac{\mathcal{E}_i}{\epsilon_i}) \leq \bar{\epsilon}_i = \zeta\epsilon_i. \tag{31}$$

will be used [7]. ϵ is a constant in respect with $\zeta = e^{-(1+\zeta)}$, *for example* 0.2785. For certain dynamics in doubly fed induction generator-based wind turbine (17), the adaptive control fuzzy can be written as

$$V_{rq} = sgn(N_1)(-\mathcal{F}_{11}\mathcal{E}_1 - \mathcal{F}_{12} Tanh\left(\frac{\mathcal{E}_1}{\epsilon_1}\right) - \theta_1^T\psi_1(x_1)). \tag{32}$$

$$V_{rd} = sgn(N_2)(-\mathcal{F}_{21}e_1 - \mathcal{F}_{22} Tanh\left(\frac{\mathcal{E}_2}{\epsilon_2}\right) - \theta_2^T\psi_2(x_1)). \tag{33}$$

As θ_i demonstrates fuzzy adjustable parameter vectors and $\psi_i(x_i)$ are fuzzy basis function vectors, proven by designer and ϵ_i are strict positive constants and $\mathcal{F}_{i1}$ are the constant parameters, the type 2 adaptive fuzzy term, $\theta_i^T\psi_i(x_i)$ will approximate the unknown functions. For estimating the unknown vectors θ_i^* and unknown parameters $\mathcal{F}_{i2}^*$ and the optional values for design constants $g_{\theta_{i(r,l)}}$, $\delta_{\theta_{i(r,l)}}$, $g_{\mathcal{F}_i}$, $\delta_{\mathcal{F}_i}$, the adaptation laws are obtained as

$$\dot{\theta}_{1l} = -\delta_{\theta_{1l}} g_{\theta_{1l}}\theta_{1l} + \frac{1}{2} g_{\theta_{1l}} \mathcal{E}_1\psi_{1l}(x_1). \tag{34}$$

$$\dot{\theta}_{1r} = -\delta_{\theta_{1r}} g_{\theta_{1r}}\theta_{1r} + \frac{1}{2} g_{\theta_{1r}} \mathcal{E}_1\psi_{1r}(x_1). \tag{35}$$

$$\dot{\theta}_{2l} = -\delta_{\theta_{2l}} g_{\theta_{2l}}\theta_{1l} + \frac{1}{2} g_{\theta_{2l}} \mathcal{E}_2\psi_{2l}(x_2). \tag{36}$$

$$\dot{\theta}_{2r} = -\delta_{\theta_{2r}} g_{\theta_{2r}}\theta_{2r} + \frac{1}{2} g_{\theta_{2r}} \mathcal{E}_2\psi_{2r}(x_2). \tag{37}$$

$$\dot{\mathcal{F}}_{12} = -\delta_{\mathcal{F}_{12}} g_{\mathcal{F}_{12}} \mathcal{F}_{12} + g_{\mathcal{F}_{12}} \mathcal{E}_1 tan\left(\frac{\mathcal{E}_1}{\epsilon_1}\right). \tag{38}$$

$$\dot{\mathcal{F}}_{22} = -\delta_{\mathcal{F}_{22}} g_{\mathcal{F}_{22}} \mathcal{F}_{22} + g_{\mathcal{F}_{22}} \mathcal{E}_2 tan\left(\frac{\mathcal{E}_2}{\epsilon_2}\right). \tag{39}$$

The design parameters such as $\mathcal{F}_{11}$, $\mathcal{F}_{21}$,$\delta_{\mathcal{F}_{12}}$,$\delta_{\mathcal{F}_{22}}$,$\epsilon_1$,$\epsilon_2$,$\delta_{\theta 1(r,l)}$,$\delta_{\theta 2(r,l)}$, $g_{\theta 1(r,l)}$,$g_{\theta 2(r,l)}$,$g_{\mathcal{F}12}$ and $g_{\mathcal{F}22}$ are optionally selected based on the Table 3.
In order to obtain the following aspects, the Lyapunov approach is formulated as (40)

a) Closed loop signal systems are bounded

b) Optimally tuning the design parameters exponentially converges the tracking errors $\mathcal{E}_1$ and $\mathcal{E}_2$ to a residual set which makes them small.

$$V = \frac{1}{2\left|N_1\right|}\mathcal{E}_1^2 + \frac{1}{2\left|N_2\right|}\mathcal{E}_2^2 + \frac{1}{2g_{\theta 1_l}}\widetilde{\theta}_{1l}^T\widetilde{\theta}_{1l} + \frac{1}{2g_{\theta 1_r}}\widetilde{\theta}_{1r}^T\widetilde{\theta}_{1r} + \frac{1}{2g_{\theta 2_l}}\widetilde{\theta}_{2l}^T\widetilde{\theta}_{2l} + \frac{1}{2g_{\theta 2_r}}\widetilde{\theta}_{2r}^T\widetilde{\theta}_{2r} + \frac{1}{2g_{k_1}}\widetilde{\mathcal{F}}_{12}^2 + \frac{1}{2g_{k_2}}\widetilde{\mathcal{F}}_{22}^2. \tag{40}$$

For ideal θ_i^* and $\mathcal{F}_{i2}^*, \widetilde{\theta}_i = \theta_i - \theta_i^*, \widetilde{\mathcal{F}}_{i2} = \mathcal{F}_{i2} - \mathcal{F}_{i2}^*$ are assumed as approximation errors.
The time derivative of the Lyapunov candidate is shown

$$\dot{V} = \frac{1}{\left|N_1\right|}\mathcal{E}_1\dot{\mathcal{E}}_1 + \frac{1}{\left|N_2\right|}\mathcal{E}_2\dot{\mathcal{E}}_2 + \frac{1}{g_{\theta 1_l}}\widetilde{\theta}_{1l}^T\dot{\widetilde{\theta}}_{1l} + \frac{1}{g_{\theta 1_r}}\widetilde{\theta}_{1r}^T\dot{\widetilde{\theta}}_{1r} + \frac{1}{g_{\theta 2_l}}\widetilde{\theta}_{2l}^T\dot{\widetilde{\theta}}_{2l} + \frac{1}{g_{\theta 2_r}}\widetilde{\theta}_{2r}^T\dot{\widetilde{\theta}}_{2r} + \frac{1}{g_{k_1}}\widetilde{\mathcal{F}}_{12}\dot{\widetilde{\mathcal{F}}}_{12} + \frac{1}{g_{k_2}}\widetilde{\mathcal{F}}_{22}\dot{\widetilde{\mathcal{F}}}_{22}. \tag{41}$$

Substituting $\dot{\mathcal{E}}_1$ and $\dot{\mathcal{E}}_2$ with (27) and (28)

$$\begin{aligned}\dot{V} = {} & \frac{1}{\left|N_1\right|}\mathcal{E}_1\left[S_1\left(x_1\right) + N_1 V_{rq}\right] + \frac{1}{\left|N_2\right|}\mathcal{E}_2\left[S_2\left(x_2\right) + N_2 V_{rd}\right] + \frac{1}{g_{\theta 1_l}}\widetilde{\theta}_{1l}^T\dot{\widetilde{\theta}}_{1l} + \frac{1}{g_{\theta 1_r}}\widetilde{\theta}_{1r}^T\dot{\widetilde{\theta}}_{1r} \\ & + \frac{1}{g_{\theta 2_l}}\widetilde{\theta}_{2l}^T\dot{\widetilde{\theta}}_{2l} + \frac{1}{g_{\theta 2_r}}\widetilde{\theta}_{2r}^T\dot{\widetilde{\theta}}_{2r} + \frac{1}{g_{k_1}}\widetilde{\mathcal{F}}_{12}\dot{\widetilde{\mathcal{F}}}_{12} + \frac{1}{g_{k_2}}\widetilde{\mathcal{F}}_{22}\dot{\widetilde{\mathcal{F}}}_{22}.\end{aligned}$$

$$\text{with } \bar{S}_1\left(x_1\right) = \left|N_1\right|^{-1} S_1\left(x_1\right) \text{ and } \bar{S}_2\left(x_2\right) = \left|N_2\right|^{-1} S_2\left(x_2\right).$$

$$\begin{aligned}\dot{V} = {} & \mathcal{E}_1[\bar{S}_1\left(x_1\right) + sgn(N_1)V_{rq}] + \mathcal{E}_2[\bar{S}_2\left(x_2\right) + sgn(N_2)V_{rd}] + \frac{1}{g_{\theta 1_l}}\widetilde{\theta}_{1l}^T\dot{\widetilde{\theta}}_{1l} + \frac{1}{g_{\theta 1_r}}\widetilde{\theta}_{1r}^T\dot{\widetilde{\theta}}_{1r} \\ & + \frac{1}{g_{\theta 2_l}}\widetilde{\theta}_{2l}^T\dot{\widetilde{\theta}}_{2l} + \frac{1}{g_{\theta 2_r}}\widetilde{\theta}_{2r}^T\dot{\widetilde{\theta}}_{2r} + \frac{1}{g_{\mathcal{F}_1}}\widetilde{\mathcal{F}}_{12}\dot{\widetilde{\mathcal{F}}}_{12} + \frac{1}{g_{\mathcal{F}_2}}\widetilde{\mathcal{F}}_{22}\dot{\widetilde{\mathcal{F}}}_{22}.\end{aligned} \tag{42}$$

If we approximate $\bar{S}_1\left(x_1\right) and \bar{S}_2\left(x_2\right)$ with the type 2 adaptive fuzzy systems in (21), (22) and use the universal approximation theorem [28] we reach to the following equations

$$\bar{S}_1\left(x_1\right) = 0.5[\theta_{r1}^{*^T} \quad \theta_{l1}^{*^T}]t[\begin{matrix}\psi_{r1}\\ \psi_{l1}\end{matrix}] + \bar{w}_1(x_1), \quad \bar{S}_2\left(x_2\right) = 0.5\begin{bmatrix}\theta_{r2}^{*^T} & \theta_{l2}^{*^T}\end{bmatrix}\begin{bmatrix}\psi_{r2}\\ \psi_{l2}\end{bmatrix} + \bar{w}_2(x_2).$$

then

$$\bar{S}_1\left(x_1\right) = 0.5\theta_{r1}^{*^T}\psi_{r1} + 0.5\theta_{l1}^{*^T}\psi_{l1} + \bar{w}_1(x_1), \quad \bar{S}_2\left(x_2\right) = 0.5\theta_{r2}^{*^T}\psi_{r2} + 0.5\theta_{l2}^{*^T}\psi_{l2} + \bar{w}_2(x_2).$$

thus

$$\begin{cases}\bar{S}_1\left(x_1\right) = 0.5\left(-\widetilde{\theta}_{1r}^T\psi_{r1} - \widetilde{\theta}_{1l}^T\psi_{l1}\right) + 0.5\left(\theta_{1r}^T\psi_{r1} + \theta_{1l}^T\psi_{l1}\right) + \bar{w}_1(x_1) \\ \bar{S}_2\left(x_2\right) = 0.5\left(-\widetilde{\theta}_{2r}^T\psi_{r2} - \widetilde{\theta}_{2l}^T\psi_{l2}\right) + 0.5\left(\theta_{2r}^T\psi_{r2} + \theta_{2l}^T\psi_{l2}\right) + \bar{w}_2(x_2)\end{cases} \tag{43}$$

$\bar{w}_i(x_i)$ is the approximation error that its bounds are adapted due to the adaptive laws in (38) ,(39) as $\bar{w}_i(x_i) \leq \mathcal{F}^*_{i2}$, [8, 9, 10, 28]. Now by combining (32)-(33) with (42), the result is demonstrated as

$$\begin{aligned}\dot{V} = &-0.5\mathcal{E}_1\widetilde{\theta}_{1r}^T\psi_{r1}(x_1) - 0.5\mathcal{E}_1\widetilde{\theta}_{1l}^T\psi_{l1}(x_1) - \mathcal{F}_{11}{\mathcal{E}_1}^2 - \mathcal{F}_{12}\mathcal{E}_1 Tanh\left(\frac{\mathcal{E}_1}{\epsilon_1}\right) + \mathcal{E}_1\bar{w}_1(x_1)\\ &-0.5\mathcal{E}_2\widetilde{\theta}_{2r}^T\psi_{r2}(x_2) - 0.5\mathcal{E}_2\widetilde{\theta}_{2l}^T\psi_{l2}(x_2) + \mathcal{E}_2\bar{w}_2(x_2) - \mathcal{F}_{21}{\mathcal{E}_2}^2 - \mathcal{F}_{22}\mathcal{E}_2 Tanh\left(\frac{\mathcal{E}_2}{\epsilon_2}\right)\\ &+\frac{1}{g_{\theta 1_l}}\widetilde{\theta}_{1l}^T\dot{\widetilde{\theta}}_{1l} + \frac{1}{g_{\theta 1_r}}\widetilde{\theta}_{1r}^T\dot{\widetilde{\theta}}_{1r} + \frac{1}{g_{\theta 2_l}}\widetilde{\theta}_{2l}^T\dot{\widetilde{\theta}}_{2l} + \frac{1}{g_{\theta 2_r}}\widetilde{\theta}_{2r}^T\dot{\widetilde{\theta}}_{2r} + \frac{1}{g_{\mathcal{F}_1}}\widetilde{\mathcal{F}}_{12}\dot{\widetilde{\mathcal{F}}}_{12} + \frac{1}{g_{\mathcal{F}_2}}\widetilde{\mathcal{F}}_{22}\dot{\widetilde{\mathcal{F}}}_{22}\end{aligned} \tag{44}$$

Therefore by $|\mathcal{E}_i\bar{w}_i(x_i)| \leq |\mathcal{E}_i|\,\mathcal{F}^*_{i2}$

$$\begin{aligned}\leq &-\mathcal{F}_{11}{\mathcal{E}_1}^2 - \mathcal{F}_{21}{\mathcal{E}_2}^2 - 0.5\mathcal{E}_1\widetilde{\theta}_{1r}^T\psi_{r1}(x_1) - 0.5\mathcal{E}_1\widetilde{\theta}_{1l}^T\psi_{l1}(x_1) - 0.5\mathcal{E}_2\widetilde{\theta}_{2r}^T\psi_{r2}(x_2) - 0.5\mathcal{E}_2\widetilde{\theta}_{2l}^T\psi_{l2}(x_2)\\ &+{\mathcal{F}^*}_{12}|\mathcal{E}_1| - \mathcal{F}_{12}\mathcal{E}_1 Tanh\left(\frac{\mathcal{E}_1}{\epsilon_1}\right) + {\mathcal{F}^*}_{22}|\mathcal{E}_2| - \mathcal{F}_{22}\mathcal{E}_2 Tanh\left(\frac{\mathcal{E}_2}{\epsilon_2}\right) + \frac{1}{g_{\theta 1_l}}\widetilde{\theta}_{1l}^T\dot{\widetilde{\theta}}_{1l}\\ &+\frac{1}{g_{\theta 1_r}}\widetilde{\theta}_{1r}^T\dot{\widetilde{\theta}}_{1r} + \frac{1}{g_{\theta 2_l}}\widetilde{\theta}_{2l}^T\dot{\widetilde{\theta}}_{2l} + \frac{1}{g_{\theta 2_r}}\widetilde{\theta}_{2r}^T\dot{\widetilde{\theta}}_{2r} + \frac{1}{g_{\mathcal{F}_1}}\widetilde{\mathcal{F}}_{12}\dot{\widetilde{\mathcal{F}}}_{12} + \frac{1}{g_{\mathcal{F}_2}}\widetilde{\mathcal{F}}_{22}\dot{\widetilde{\mathcal{F}}}_{22}\end{aligned} \tag{45}$$

Extending the equation (45) by considering the inequality in (31):

$$\begin{aligned}\dot{V} \leq &-\mathcal{F}_{11}{\mathcal{E}_1}^2 - \mathcal{F}_{21}{\mathcal{E}_2}^2 - 0.5\mathcal{E}_1\widetilde{\theta}_{1r}^T\psi_{r1}(x_1) - 0.5\mathcal{E}_1\widetilde{\theta}_{1l}^T\psi_{l1}(x_1) - 0.5\mathcal{E}_2\widetilde{\theta}_{2r}^T\psi_{r2}(x_2) - 0.5\mathcal{E}_2\widetilde{\theta}_{2l}^T\psi_{l2}(x_2)\\ &-\mathcal{F}_{12}\mathcal{E}_1 Tanh\left(\frac{\mathcal{E}_1}{\epsilon_1}\right) + {\mathcal{F}^*}_{22}|\mathcal{E}_2| - \mathcal{F}_{22}\mathcal{E}_2 Tanh\left(\frac{\mathcal{E}_2}{\epsilon_2}\right) + \frac{1}{g_{\theta 1_l}}\widetilde{\theta}_{1l}^T\dot{\widetilde{\theta}}_{1l} + \frac{1}{g_{\theta 1_r}}\widetilde{\theta}_{1r}^T\dot{\widetilde{\theta}}_{1r}\\ &+\frac{1}{g_{\theta 2_l}}\widetilde{\theta}_{2l}^T\dot{\widetilde{\theta}}_{2l} + \frac{1}{g_{\theta 2_r}}\widetilde{\theta}_{2r}^T\dot{\widetilde{\theta}}_{2r} + \frac{1}{g_{\mathcal{F}_1}}\widetilde{\mathcal{F}}_{12}\dot{\widetilde{\mathcal{F}}}_{12} + \frac{1}{g_{2\mathcal{F}_2}}\widetilde{\mathcal{F}}_{22}\dot{\widetilde{\mathcal{F}}}_{22} + \mathcal{F}^*_{12}\bar{\epsilon}_1 + \mathcal{F}^*_{22}\bar{\epsilon}_2\end{aligned} \tag{46}$$

$$\begin{aligned}\leq &-\mathcal{F}_{11}{\mathcal{E}_1}^2 - \mathcal{F}_{21}{\mathcal{E}_2}^2 + \frac{1}{2g_{\theta 1_r}}\widetilde{\theta}_{1r}^T\left(2\dot{\widetilde{\theta}}_{1r} - g_{\theta 1_r}\mathcal{E}_1\psi_{r1}(x_1)\right) + \frac{1}{2g_{\theta 1_l}}\widetilde{\theta}_{1l}^T\left(2\dot{\widetilde{\theta}}_{1l} - g_{\theta 1_l}\mathcal{E}_1\psi_{l1}(x_1)\right)\\ &+\frac{1}{g_{\mathcal{F}_{12}}}\widetilde{\mathcal{F}}_{12}\left(\dot{\mathcal{F}}_{12} - g_{k_{12}}\mathcal{E}_1 Tanh\left(\frac{\mathcal{E}_1}{\epsilon_1}\right)\right) + \frac{1}{2g_{\theta 2_r}}\widetilde{\theta}_{2r}^T\left(2\dot{\widetilde{\theta}}_{2r} - g_{\theta 2_r}\mathcal{E}_2\psi_{r2}(x_2)\right) + \frac{1}{2g_{\theta 2_l}}\widetilde{\theta}_{2l}^T\left(2\dot{\widetilde{\theta}}_{2l}\right.\\ &\left.-g_{\theta 2_l}\mathcal{E}_2\psi_{l2}(x_2)\right) + \frac{1}{g_{\mathcal{F}_{22}}}\widetilde{\mathcal{F}}_{22}\left(\dot{\mathcal{F}}_{22} - g_{k_{22}}\mathcal{E}_2 Tanh\left(\frac{\mathcal{E}_2}{\epsilon_2}\right)\right) + \mathcal{F}^*_{12}\bar{\epsilon}_1 + \mathcal{F}^*_{22}\bar{\epsilon}_2\end{aligned} \tag{47}$$

Employing the adaptation laws in (34)-(39), turns (48) to

$$\begin{aligned}\dot{V} \leq &-\mathcal{F}_{11}{\mathcal{E}_1}^2 - \mathcal{F}_{21}{\mathcal{E}_2}^2 - \delta_{\theta_{1l}}\widetilde{\theta}_{1l}^T\widetilde{\theta}_{1l} - \delta_{\theta_{1r}}\widetilde{\theta}_{1r}^T\widetilde{\theta}_{1r} - \delta_{\theta_{2l}}\widetilde{\theta}_{2l}^T\widetilde{\theta}_{2l}\\ &-\delta_{\theta_{2r}}\widetilde{\theta}_{2r}^T\widetilde{\theta}_{2r} - \delta_{k_1}\widetilde{\mathcal{F}}_{12}\mathcal{F}_{12} - \delta_{k_2}\widetilde{\mathcal{F}}_{22}\mathcal{F}_{22} + \mathcal{F}^*_{12}\bar{\epsilon}_1 + \mathcal{F}^*_{22}\bar{\epsilon}_2\end{aligned} \tag{48}$$

Defining the following concept

$$\begin{cases}-\delta_{\theta_{(r,l)i}}\widetilde{\theta}_{(r,l)i}^T\theta_{(r,l)i} \leq -0.5\delta_{\theta_{(r,l)i}}\|\widetilde{\theta}_{(r,l)i}\|^2 + 0.5\delta_{\theta(r,l)i}\|\theta^*_{(r,l)i}\|^2\\ -\delta_{\mathcal{F}_{i2}}\widetilde{\mathcal{F}}_{i2}\mathcal{F}_{i2} \leq -0.5\delta_{\mathcal{F}_{i2}}\widetilde{\mathcal{F}}^2_{i2} + 0.5\delta_{\mathcal{F}_{i2}}\widetilde{\mathcal{F}}^{*2}{}_{i2} \qquad i = 1, 2\end{cases}$$

The resulted equation (48), changes to

$$\begin{aligned}\dot{V} \leq &-\mathcal{F}_{11}{\mathcal{E}_1}^2 - \mathcal{F}_{21}{\mathcal{E}_2}^2 - 0.5\delta_{\theta_{l1}}\|\widetilde{\theta}_{l1}\|^2 - 0.5\delta_{\theta_{r1}}\|\widetilde{\theta}_{r1}\|^2 - 0.5\delta_{\theta_{l2}}\|\widetilde{\theta}_{l2}\|^2 - 0.5\delta_{\theta_{r2}}\|\widetilde{\theta}_{r2}\|^2 + 0.5\delta_{\mathcal{F}_{12}}\widetilde{\mathcal{F}}^2_{12}\\ &+ 0.5\delta_{\mathcal{F}_{22}}\widetilde{\mathcal{F}}^2_{22} + \mathcal{F}^*_{12}\bar{\epsilon}_1 + \mathcal{F}^*_{22}\bar{\epsilon}_2 + 0.5\delta_{\theta_{l1}}\|\theta^*_{l1}\|^2 + 0.5\delta_{\theta_{r1}}\|\theta^*_{r1}\|^2 + 0.5\delta_{\theta_{l2}}\|\theta^*_{l2}\|^2\\ &+ 0.5\delta_{\theta_{r2}}\|\theta^*_{r2}\|^2 + 0.5\delta_{\mathcal{F}_{12}}\widetilde{\mathcal{F}}^{*2}{}_{12} + 0.5\delta_{\mathcal{F}_{22}}\widetilde{\mathcal{F}}^{*2}{}_{22}.\end{aligned} \tag{49}$$

Considering

$$\mathcal{Z} = \mathcal{F}_{12}^{*}\bar{\epsilon}_1 + \mathcal{F}_{22}^{*}\bar{\epsilon}_2 + 0.5\delta_{\theta_{l1}}\|\theta_{l1}^{*}\|^2 + 0.5\delta_{\theta_{r1}}\|\theta_{r1}^{*}\|^2 + 0.5\delta_{\theta_{l2}}\|\theta_{l2}^{*}\|^2 + 0.5\delta_{\theta_{r2}}\|\theta_{r2}^{*}\|^2 + 0.5\delta_{\mathcal{F}_{12}}\widetilde{\mathcal{F}}^{*2}{}_{12} + 0.5\delta_{\mathcal{F}_{22}}\widetilde{\mathcal{F}}^{*2}{}_{22}. \tag{50}$$

Simplifying (49), we reach

$$\dot{V} \leq -\mathcal{J}V + \mathcal{Z} if \mathcal{J} = \min\{2\left|N_1\right|\mathcal{F}_{11}, 2\left|N_2\right|\mathcal{F}_{21}, \delta_{\theta_{l1}}g_{\theta l_1}, \delta_{\theta_{r1}}g_{\theta r_1}, \delta_{\theta_{l2}}g_{\theta_{l2}}, \delta_{\theta_{r2}}g_{\theta_{r2}}, \delta_{\mathcal{F}_{12}}g_{k\mathcal{F}_{12}}, \delta_{\mathcal{F}_{22}}g_{\mathcal{F}_{22}}\}. \tag{51}$$

Then we can rewrite (51) as below

$$\frac{d}{dt}(e^{\mathcal{J}}V) \leq \mathcal{Z}e^{\mathcal{J}t}. \tag{52}$$

By merging (52) into $[0, t]$, the result will be

$$0 \leq V(t) \leq \frac{\mathcal{Z}}{\mathcal{J}} + (V(0) - \frac{\mathcal{Z}}{\mathcal{J}})e^{-\mathcal{J}t}. \tag{53}$$

□

It can be seen, the parameter $\mathcal{J}$ strictly depends on the given design parameter values in Table.3. Based on (51), $\mathcal{J}$ as calculated to be 10^{-6}. Generally, for the smaller values of $\mathcal{J}$, the Lyapunov will converge to zero more quickly. Since, the $\frac{\mathcal{Z}}{\mathcal{J}}$ will get high values, therefore $0 \leq V(t) \leq \frac{\mathcal{Z}}{\mathcal{J}}$ obviously proves that the Lyapunov candidate is uniformly ultimately bounded. Due to selecting an arbitrary value for g and knowing the dependence of $\mathcal{J}$ on design parameters, the tracking errors will stand in arbitrary small bounds. It must be cited that the boundness of $\theta_1, \theta_2, \mathcal{F}_{12}$ *and* $\mathcal{F}_{22}$ is determined by $\widetilde{\theta}_1, \widetilde{\theta}_2, \widetilde{\mathcal{F}}_{12}, \widetilde{\mathcal{F}}_{22}$. Ultimately, the requirements of uniformly ultimately boundness stabilization for tracking errors $\mathcal{E}_1$, $\mathcal{E}_2$ and also the parameter approximation errors $\widetilde{\theta}_1, \widetilde{\theta}_2, \widetilde{\mathcal{F}}_{12}, \widetilde{\mathcal{F}}_{22}$ are met [10].

5 Simulation results

Simulating the above described system results in the presented outputs, it is required to consider the following values for the parameters of wind turbine and doubly fed induction generator system according to the proposed technique in [14]:

Table 2: Parameters of DFIG and WT [14]

Parameters	Value
No of blades	3
Turbine radius	3 m
Gearbox (G)	8
Max value to $C_P(C_{P_{max}})$	0.48
Rated Power (P_{rated})	7.5 KW
Sync Speed (ω_{sn})	$2\pi 50$ Hz
Rotor resistance (R_r)	0.620 Ω
Stator resistance (R_s)	0.455 Ω
Stator inductance (L_s)	0.084 H
Rotor inductance (L_r)	0.081 H
Mutual inductance (M)	0.078 H
Pole pairs (P)	2
Total inertia ($\mathcal{H}_t$)	0.3125 kgm^2
Viscous friction coefficient (μ_{fr})	0.014 $Nm.s/rad$
Coulomb friction coefficient (μ_{stc})	0.07 Nm
Static friction coefficient (μ_{cmb})	0.1 Nm
Static friction decreasing rate (η_s)	0.02 rad/s

Considering $x1$ and $x2$ as system inputs, for each input variables we dedicate three trapezoidal membership functions distributed on specified intervals. These intervals are different for each variable as following: $[-25, 25]$ for i_{rd} and i_{rq}, $[0, 100]$ for $\mathcal{T}_{ar}$ and $[0, 200]$ for Ω. The design parameters are optionally chosen, as below;

Table 3: Chosen design parameter values

Parameters	Value
$\mathcal{F}_{11} = 1200$	$\mathcal{F}_{21} = 1500$
$\epsilon_1 = 0.1$	$\epsilon_2 = 1$
$\delta_{\theta 1(r,l)} = 10^{-3}$	$\delta_{\theta 2(r,l)} = 10^{-3}$
$\delta_{\mathcal{F}_{12}} = 10^{-5}$	$\delta_{\mathcal{F}_{22}} = 10^{-5}$
$g_{\theta 1(r,l)} = 100$	$g_{\theta 2(r,l)} = 100$
$g_{\mathcal{F}11} = 0.1$	$g_{\mathcal{F}22} = 0.1$

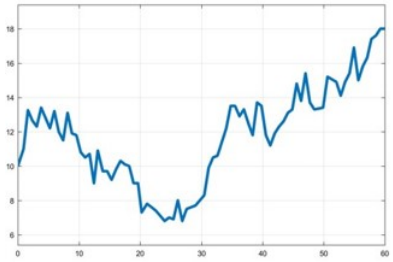

Figure 5: Wind speed variation profile

The operation of the system as shown in Figures 6-11. Also, a brief comparison is conducted between type 1 adaptive fuzzy control ($T1AFC$) and type 2 adaptive fuzzy systems ($T2AFC$). This comparison is made by Mean Square Error (MSE) which can be calculated by (54).

$$\text{Mean Square Error(MSE)} \;=\; \frac{1}{n}\sum (y-\hat{y})^{2}. \tag{54}$$

The electromagnetic torque and aerodynamic torque are clearly indicated in Figure 6. Obviously declared, the type two adaptive fuzzy system approaches to the reference value more adequately, as the undershoot is much smaller in it, compared with the type one adaptive control system. Based on (54), the MSE for the error proposed in (23) is 2.11×10^{-55}, in contrast, the MSE for T1AFC gets the value of 2.48×10^{-27}. This comparison shows the functionality of $T2AFC$ is more acceptable rather than $T1AFC$. Moreover, the adaptation time is less in $T2AFC$ (8×10^{-5} s) than $T1AFC$ (1.9×10^{-4} s).

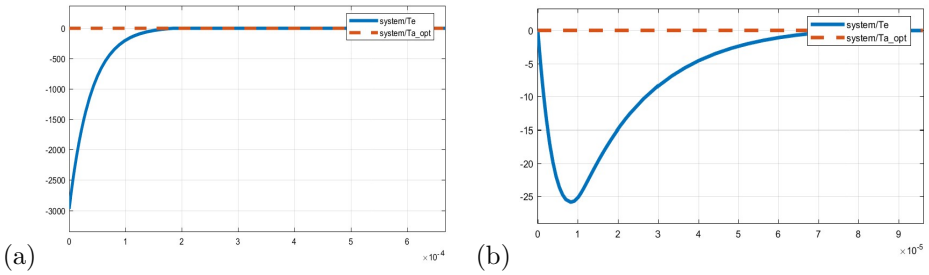

(a) (b)

Figure 6: Torque tracking error (a) $T1AFC$ ($MSE = 2.48 \times 10^{-27}$), ($b$) $T2AFC$ ($MSE = 2.11 \times 10^{-55}$)

Unlike the T2AFC, it can be seen in Figure 7, the d-reference rotor side current over passes the reference current value in $T1AFC$ and I cant converge to the reference value. Completely different from $T1AFC$ with $MSE = 4.49 \times 10^{-2}$, the calculated MSE for $T2AFC$ equals to 2.73×10^{-6}. Ignoring the malfunction of $T1AFC$ to track the optimal values, a new comparison is conducted between these two methods. Shown in Figure 7, the i_{rd} will be adapted faster in $T2AFC$ ($\approx 1.25 \times 10^{-5}$ s) rather than T1AFC ($\approx 2 \times 10^{-5}$ s).

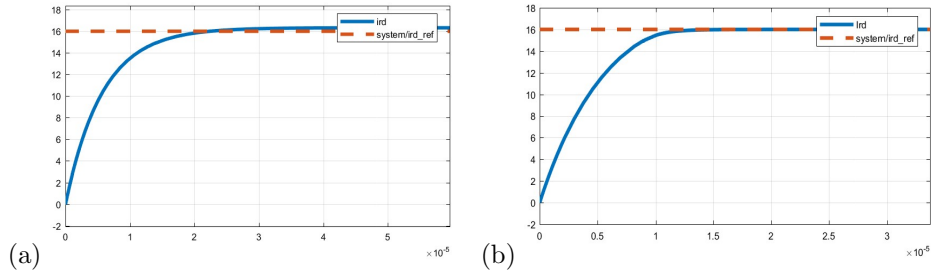

(a) (b)

Figure 7: d-axis rotor current tracking error (a) $T1AFC$ $(MSE = 4.49 \times 10^{-2})$, (b) $T2AFC(MSE = 2.73 \times 10^{-6})$

Illustrated in Figure 8, the generated power is compared for two proposed control techniques. It can be seen that the wind turbine produces higher power value by $T2AFC$ in contrast with $T1AFC$.

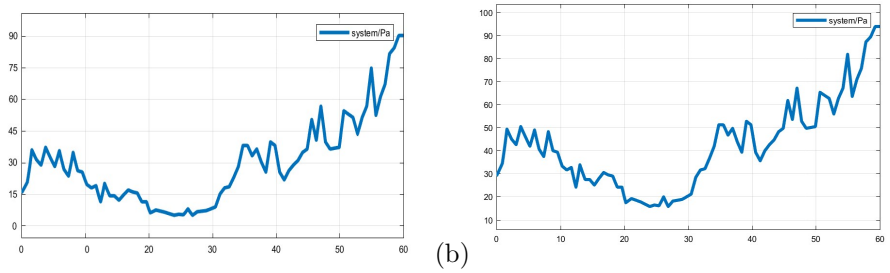

(a) (b)

Figure 8: Generated aerodynamic power (a) $T1AFC$, (b) $T2AFC$

In theorical bases, it was described that the stator reactive power must be zero. Presented in Figure 9, the application of T2AFC helps to keep the stator reactive power at zero. Based on (2), the power coefficient is shown in Figure 10.

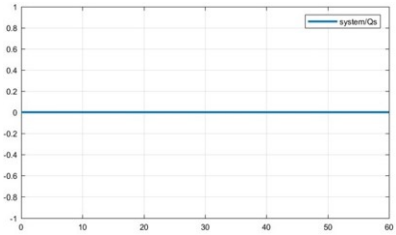

Figure 9: Stator reactive power $(T2AFC)$

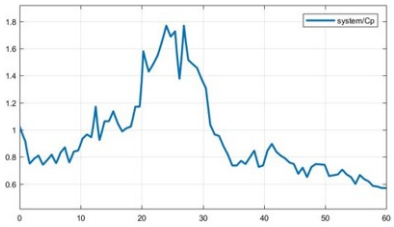

Figure 10: Power coefficient $(T2AFC)$

Different factors such as parameter variations, existing dynamics may affect the system operation, but the proposed control approaches $(T2AFCandT1AFC)$ show a chattering free behavior as indicated in Figure 11.

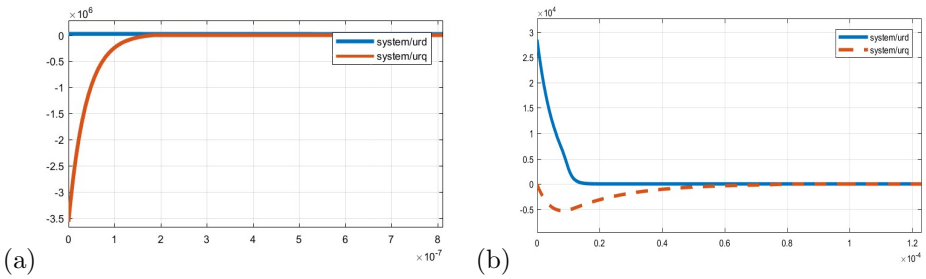

(a) (b)

Figure 11: Rotor control inputs (*a*) $T1AFC$, (*b*) $T2AFC$

6 Conclusion

In presence of wind speed variations, an efficient wind turbine system is the one that is capable to transform the majority of mechanical energy into the current values by the application of a doubly fed induction generator. In this paper, the possibility of implementing the type 2 adaptive fuzzy control approach to a grid-connected variable speed DFIG-based wind turbine is assessed in detail. This assessment is conducted by given models and parameters. The control objectives are described as: Extracting the maximum power from the wind, derived from the aerodynamics and electromagnetic torques adaptation, and based on the grid needs, and the power factor must be fixed to an optimal value. Thanks to the proposed control approach, the extracted current and the calculated electromagnetic torque track the optimal aerodynamic torque value (Maximum Power Point Tracking Algorithm). The type two fuzzy system adequately approximates the nonlinearities, appeared in the tracking errors, and the uncertainties such as speed variations influencing the system behavior. All these issues are performed by considering the parameter variations and frictional influences. Furthermore, the Lyapunov stability analysis technique is used to produce the best adaptation laws for the controlling methods to adapt the adjustable fuzzy parameters. This system is robust enough to operate in presence of model uncertainties such as unknown parameters (structured uncertainties) and/or disturbances (unstructured uncertainties). Achieved from the simulations, and the comparison made between $T2AFC$ and $T1AFC$, the presented approach operates better than $T1AFC$. It also proved that parameter approximation and tracking errors meet UUB stability. Also, it is tried to maintain the stator side reactive power at zero to satisfy the power unity factor. Consequently, this novel type 2 adaptive fuzzy control technique guarantees the robustness and stability of the system.

References

[1] S. Andersson, A. Söderberg, S. Björklund, *Friction models for sliding dry, boundary and mixed lubricated contacts*, Tribology International, **40**(4) (2007), 580-587.

[2] A. Bektache, B. Boukhezzar, *Nonlinear predictive control of a DFIG-based wind turbine for power capture optimization*, International Journal of Electrical Power and Energy Systems, **101** (2018), 92-102.

[3] B. Beltran, M. E. H. Benbouzid, T. Ahmed-Ali, *High-order sliding mode control of a DFIG-based wind turbine for power maximization and grid fault tolerance*, Conference: Electric Machines and Drives Conference, 2009. IEMDC '09. IEEE International, 2009.

[4] B. Beltran, M. E. H. Benbouzid, T. Ahmed-Ali, *Second-order sliding mode control of a doubly-fed induction generator driven wind turbine*, IEEE Transactions on Energy Conversion, **27**(2) (2012), 261-269.

[5] Z. Boudjema, A. Meroufel, E. Bounadja, Y. Djeriri, *Nonlinear control of a doubly-fed induction generator supplied by a matrix converter for wind energy conversion systems*, Journal of Electrical Engineering, **13** (2013), 60-68.

[6] Z. Boudjema, T. Rachid, Y. Djeriri, A. Yahdou, *A novel direct torque control using second order continuous sliding mode of a doubly-fed induction generator for a wind energy conversion system*, Turkish Journal of Electrical Engineering and Computer Sciences, **25** (2017), 965-975.

[7] B. Boukhezzar, H. Siguerdidjane, *Nonlinear control of a variable-speed wind turbine using a two-mass model*, IEEE Transactions on Energy Conversion, **26** (2011), 149-162.

[8] A. Boulkroune, N. Bounar, M. M′Saad, M. Farza, *Indirect adaptive fuzzy control scheme based on observer for nonlinear systems: A novel SPR-filter approach*, Neurocomputing, **135** (2014), 378-387, Doi: 10.1016/j.neucom.2013.12.011.

[9] A. Boulkroune, M. M′Saad, H. Chekireb, *Design of a fuzzy adaptive controller for MIMO nonlinear time-delay systems with unknown actuator nonlinearities and unknown control direction*, Information Sciences, **180**(24) (2010), 5041-5059.

[10] A. Boulkroune, M. Tadjine, M. M′Saad, M. Farza, *How to design a fuzzy adaptive controller based on observers for uncertain affine nonlinear systems*, Fuzzy Sets and Systems, **159**(8) (2008), 926-948.

[11] E. Bounadja, A. Djahbar, Z. Boudjema, *Variable structure control of a doubly-fed induction generator for wind energy conversion systems*, Energy Procedia, **50** (2014), 999-1007.

[12] N. Bounar, A. Boulkroune, F. Boudjema, *Adaptive fuzzy control of doubly-fed induction machine*, Control Engineering and Applied Informatics, **16** (2014), 98-110.

[13] N. Bounar, A. Boulkroune, F. Boudjema, M. M′Saad, M. Farza, *Adaptive fuzzy vector control for a doubly-fed induction motor*, Neurocomputing, **151** (2015), 756-769.

[14] N. Bounar, S. Labdai, A. Boulkroune, M. Farza, M. M′Saad, *Adaptive fuzzy control scheme for variable-speed wind turbines based on a doubly-fed induction generator*, Iranian Journal of Science and Technology, Transactions of Electrical Engineering, **44** (2020), 629-641.

[15] H. Chaoui, P. Sicard, *Adaptive fuzzy logic control of permanent magnet synchronous machines with nonlinear friction*, IEEE Transactions on Industrial Electronics, **59**(2) (2012), 1123-1133.

[16] M. Ghaemi, M. R. Akbarzadeh Totonchi, *Indirect adaptive interval type-2 PI sliding mode control for a class of uncertain nonlinear systems*, Iranian Journal of Fuzzy Systems, **11**(5) (2014), 1-21.

[17] B. Kiruthiga, *Implementation of first order sliding mode control of active and reactive power for DFIG based wind turbine*, International Journal of Informative and Futuristic Research, **2**(8) (2015), 2487-2497.

[18] X. Liu, Y. Han, C. Wang, *Second-order sliding mode control for power optimisation of DFIG-based variable speed wind turbine*, IET Renewable Power Generation, **11**(2) (2017), 408-418.

[19] M. I. Martinez, A. Susperregui, G. Tapia, *Second-order sliding-mode-based global control scheme for wind turbine-driven DFIGs subject to unbalanced and distorted grid voltage*, IET Electric Power Applications, **11**(6) (2017), 1013-1022.

[20] J. W. Moon, J. Gwon, J. W. Park, D. W. Kang, J. M. Kim, *Feedback linearization control of doubly-fed induction generator under an unbalanced voltage*, 8th International Conference on Power Electronics - ECCE Asia, (2011), 662-669.

[21] K. A. Naik, C. P. Gupta, E. Fernandez, *Design and implementation of interval type-2 fuzzy logic-PI based adaptive controller for DFIG based wind energy system*, International Journal of Electrical Power and Energy Systems, **115** (2020), 105468.

[22] F. A. Okou, O. Akhrif, M. Tarbouchi, *Design of a nonlinear robust adaptive controller for a grid-connected doubly-fed induction generator wind turbine*, in 18th Mediterranean Conference on Control and Automation, MED10, (2010), 1603-1608.

[23] F. Poitiers, T. Bouaouiche, M. Machmoum, *Advanced control of a doubly-fed induction generator for wind energy conversion*, Electric Power Systems Research, **79** (2009), 1085-1096.

[24] M. M. Polycarpou, P. A. Ioannou, *A robust adaptive nonlinear control design*, in 1993 American Control Conference, (1993), 1365-1369.

[25] A. Sid Ahmed El Mehdi, M. ABID, *Fuzzy sliding mode control applied to a doubly fed induction generator for wind turbines*, Turkish Journal of Electrical Engineering and Computer Sciences, **23** (2015), 1673-1686, Doi: 10.3906/elk-1404-64.

[26] O. Soares, H. Gonçalves, A. Martins, A. Carvalho, *Nonlinear control of the doubly-fed induction generator in wind power systems*, Renewable Energy, **35**(8) (2010), 1662-1670.

[27] A. Tohidi, H. Hajieghrary, M. A. Hsieh, *Adaptive disturbance rejection control scheme for DFIG-based wind turbine: Theory and experiments*, IEEE Transactions on Industry Applications, **52**(3) (2016), 2006-2015.

[28] L. X. Wang, *Adaptive fuzzy systems and control: Design and stability analysis*, Prentice-Hall, 1994.

[29] B. Yang, L. Jiang, L. Wang, W. Yao, Q. H. Wu, *Nonlinear maximum power point tracking control and modal analysis of DFIG based wind turbine*, International Journal of Electrical Power and Energy Systems, **74** (2016), 429-436.

[30] B. Yang, X. Zhang, T. Yu, H. Shu, Z. Fang, *Grouped grey wolf optimizer for maximum power point tracking of doubly-fed induction generator based wind turbine*, Energy Conversion and Management, **133** (2017), 427-443.